Detailed Electrochemical Characterisation of Large SOFC Stacks

Mosbæk, Rasmus Rode; Hjelm, Johan; Barfod, R.; Høgh, Jens Valdemar Thorvald; Hendriksen, Peter Vang

Published in:
Proceedings of 10th European SOFC Forum

Publication date:
2012

Document Version
Publisher's PDF, also known as Version of record

B1006

Detailed electrochemical characterisation of large SOFC stacks

R. R. Mosbæk (1), J. Hjelm (1), R. Barfod (2), J. Høgh (1), and P. V. Hendriksen (1)
(1) DTU Energy Conversion, Risø Campus
Frederiksborgvej 399, DK-4000, Denmark
(2) Topsoe Fuel Cell A/S, Nymøllevej 66, DK-2800 Lyngby, Denmark
Tel.: +45-4677-5669
Fax: +45-4677-5858
rasmo@dtu.dk

Abstract

As solid oxide fuel cell (SOFC) technology is moving closer to a commercial break through, lifetime limiting factors, determination of the limits of safe operation and methods to measure the “state-of-health” of operating cells and stacks are becoming of increasing interest. This requires application of advanced methods for detailed electrochemical characterisation during operation. An operating stack is subject to steep compositional gradients in the gaseous reactant streams, and significant temperature gradients across each cell and across the stack, which makes it a complex system to analyse in detail. Today one is forced to use mathematical modelling to extract information about existing gradients and cell resistances in operating stacks, as mature techniques for local probing are not available. This type of spatially resolved information is essential for model refinement and validation, and helps to further the technological stack development. Further, more detailed information obtained from operating stacks is essential for developing appropriate process monitoring and control protocols for stack and system developers.

An experimental stack with low ohmic resistance from Topsoe Fuel Cell A/S was characterised in detail using electrochemical impedance spectroscopy.
An investigation of the optimal geometrical placement of the current probes and voltage probes was carried out in order to minimise measurement errors caused by stray impedances. Unwanted stray impedances are particularly problematic at high frequencies. Stray impedances may be caused by mutual inductance and stray capacitance in the geometrical set-up and do not describe the fuel cell. Three different stack geometries were investigated by electrochemical impedance spectroscopy.

Impedance measurements were carried out at a range of ac perturbation amplitudes in order to investigate linearity of the response and the signal-to-noise ratio. Separation of the measured impedance into series and polarisation resistances was possible.

1. Introduction

The DOE lifetime target for Solid Oxide Fuel Cells (SOFCs) stacks is 60,000 h by 2020 for stationary applications [1]. Understanding and mitigation of the degradation mechanisms in SOFC stacks is therefore crucial in order to improve the durability and increase the stack lifetime [2].

Electrochemical Impedance Spectroscopy (EIS), is a powerful diagnostic technique that can increase understanding of the degradation mechanisms dominating in operating stacks since the technique may provide information on individual losses, including oxygen reduction reaction kinetics, mass-transport processes, and electrolyte resistance loss [3]. EIS has been an increasingly popular diagnostic technique at the SOFC single cell level but has so far only seen limited use on the stack level [4–7].

One of the key challenges in associated with impedance measurements of large area objects, such as the experimental SOFC stack considered here, is that the absolute real impedance for a cell in the experimental stack is in the range of a few mΩ which requires equipment with high precision and minimisation of unwanted stray impedances in the geometrical set-up. Stray impedances are caused by mutual inductance and stray capacitance and do not describe the fuel cell. Three different stack geometries were investigated by electrochemical impedance spectroscopy for stray impedance minimisation. Furthermore active electrical circuits were attached the measurement input in order to ensure the highest measurement resolution of the frequency response analyser.

In the present work, the durability of an experimental 13-cell stack, in which the metallic interconnects were coated with different types of protective layers, has been tested for more than 2500 hours at steady operating conditions. EIS has been used to examine the long-term behaviour and monitor the evolution of series and polarisation resistances for four out of the 13 cells. The losses for the four cells are reported and discussed.

2. Experiments

The solid oxide fuel cells (SOFC) used for the 13-cell experimental fuel cell stack were planar anode-supported SOFCs (Ni-YSZ/YSZ/LSM-YSZ) of 12 cm x 12 cm footprint and an active area of approximately 90 cm2. The cell details can be found elsewhere [8]. The interconnects were made of commercial stainless steel. Different coatings was used on the interconnects in the stack (see Table 1) to prevent chromium poisoning on the cathode side [9]. The nickel oxide in the Ni-YSZ electrode was reduced to nickel in hydrogen at start-up and the stack was subsequently tested for performance and durability. The stack testing was performed at DTU Energy Conversion with an experimental stack manufactured by Topsoe Fuel Cell A/S (TOFC).

Table 1: Cell number and the corresponding interconnect (IC) coating towards the cathode side. Abbreviations: Wet sprayed, ws Standard ceramic coat, st.cer.coat

Cell	IC Coating	Cell	IC Coating	Cell	IC Coating
1	st.cer.coat	6	Cu	11	Cu LSM ws
2	st.cer.coat	7	LSM ws	12	Cu
3	Co	8	st.cer.coat	13	Co
4	Co LSM ws	9	LSM ws		
5	Cu LSM ws	10	Co LSM ws		

An investigation of the optimal geometrical placement of the current probes and voltage probes was carried out in order to minimise measurement errors caused by stray impedances. Unwanted stray impedances are particularly problematic at high frequencies. The optimal stack geometry was found by performing EIS on three different stacks. The three different stack geometries are shown in Figure 1. For configuration A there was big difference in the high frequency response between the different cells in the stack since the magnetic field from the current conduction was influencing the voltage probes and causing a greater measurement error (greater stray impedance). Configuration B improved the high frequency response, but there was still a large deviation in the high frequency response between different cells in the stack. In configuration C the current conduction (out of the plane) was perpendicular to the voltage probes to minimise stray impedances as much as possible. This gave a consistent high frequency response between the different cells and decreased stray impedances. The experimental stack was therefore assembled with configuration C.

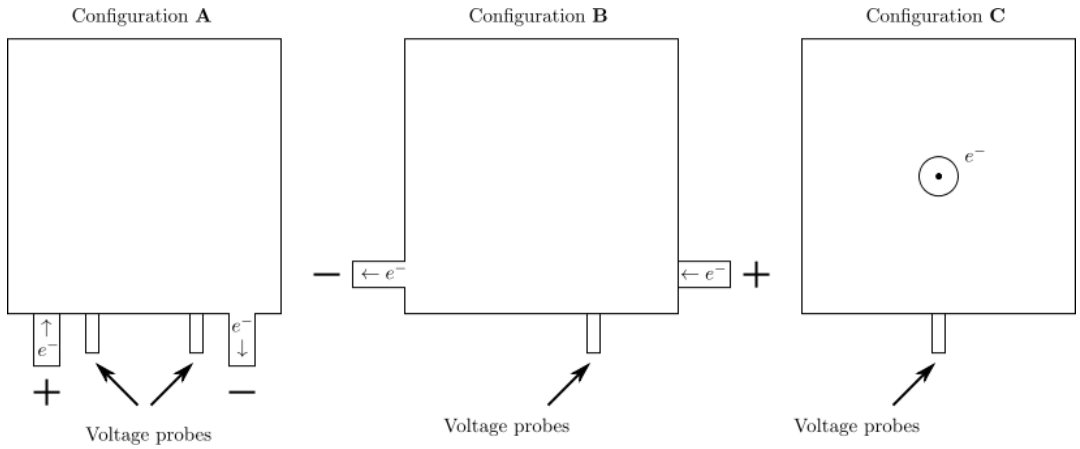

Figure 1: Three stack configurations shown from above. e⁻ indicate the current conduction. The current conduction direction for configuration C is out of the plane.

The stack was sealed along the edges with a glass seal designed by TOFC. The fuel cell stack can be considered to consist of a number of repeating units (RU). Each repeating unit contains interconnects, glass seals and a cell. A schematic representation of the experimental stack is shown in Figure 2.

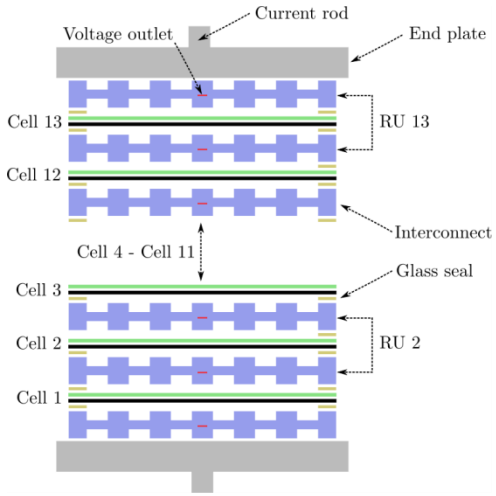

Figure 2: Schematic representation of the experimental stack.

The stack was tested using an automated test rig purchased from a commercial supplier. The stack was characterised using Electrochemical Impedance Spectroscopy (EIS). An illustration of the impedance custom test set-up is shown in figure 2. The EIS computer controls the Solartron 1260 Frequency Response Analyzer (FRA), via a GPIB communication bus. The Solartron 1260 sends an AC voltage signal from the generator output to the programmable input (Prg. Input) of a Kepco Bipolar Operational Amplifier 20-20D (Kepco Op-Amp) . The Kepco Op-Amp converts the AC voltage signal to a corresponding AC current signal with a current-to-voltage ratio of 1 A/V. The generated AC current through the SOFC stack is superimposed on the DC current provided by the Electronic load of the test stand. Four terminal measurements were used to measure the (time-dependent) currents and voltages of the RUs. The voltage of a RU was measured by a differential probe connected to the differential input V1 on the Solartron 1260. The current through the stack was measured with an active current transducer (LEM ITN-600) which has a linear response up to 200 kHz. The DC voltage and the common mode voltage was minimised by additional active electrical circuits in order to utilise the highest measurement resolution on the Solartron.

EIS spectra were recorded from 97 kHz to 0.3 Hz with an ac current modulation of 0.8 A at OCV or on top of the nominal dc current of 18.5 A during the galvanostatic long term degradation test. The AC current amplitude was selected by testing four different current amplitudes (0.25A, 0.5A, 1A and 3A). The linear Kramers-Kronig transform test was used for immittance data validation producing residuals within a range of ±2% and a χ^2 in the range of $9.1 \cdot 10^{-5}$ to $10 \cdot 10^{-5}$ [10].

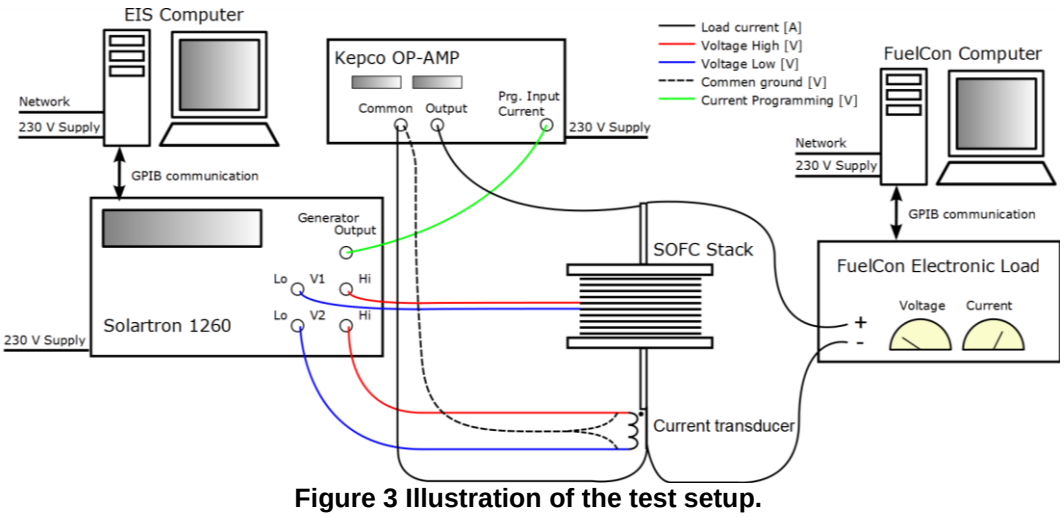

Figure 3 Illustration of the test setup.

Before the long term degradation test the stack was characterised with fuel consisting of H_2 with 20% H_2O at 700, 750 and 800˚C in order to establish the temperature dependence of the losses in the stack. Temperature monitoring was performed with type S (Pt/Pt-Rh) thermocouples for the fuel and oxidant inlet at the top and bottom end-plates. The long term degradation test was carried out at constant current (galvanostatic) conditions at 0.2 A cm^{-2} (18.5 A) and the stack temperature set to 750˚C. The fuel was H_2 with 4% H_2O the oxidant was air. After 200 h, 4% H_2O was added to the air. The fuel and oxygen utilisation was 52% and 19%, respectively.

3. Results

3.1 Initial performance

Figure 4 shows the initial performance and scattering in resistance of the different cells in the stack measured by EIS. The series resistance, R_s and the polarisation resistance R_p are derived from the EIS data and the cells are grouped in colours which represent the different coatings. The R_s and R_p data presented here were extracted from the real part of the impedance at the highest and lowest frequency. The RUs with the standard ceramic coat has the lowest total resistance, yields the lowest R_p values, and also exhibits among the smallest cell-to-cell variations. The RUs with Cu LSM wet spray coating (cells 5 and 11) has a low R_s value but a high R_p value.

The large scatter in R_s and R_p values for the different cells is likely due to that the stack is an experimental stack optimised for electrochemical impedance spectroscopy, which in this case resulted in a different pressure (compressive force) distribution compared to a standard stack.

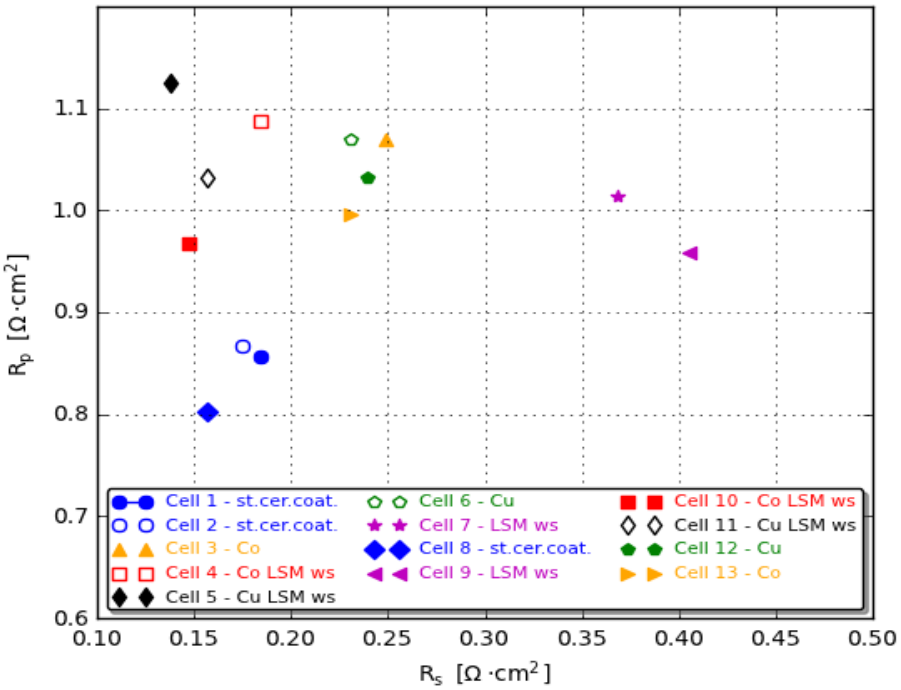

Figure 4 Initial performance of the cells in the stack measured at OCV with EIS.

Due to the time-consuming nature of the impedance characterisation carried out, not helped by the largely manual multiplexing between cells, four cells were selected for detailed analysis impedance analysis and degradation mode tracking. The cells (#2,4,6,11) were selected based on physical placement in the stack, and on the interconnect coating material. The temperature dependence in R_s and R_p for the four cells

of interest is shown in Figure 5. The corresponding activation energies for R_s and R_p are shown in Table 2.

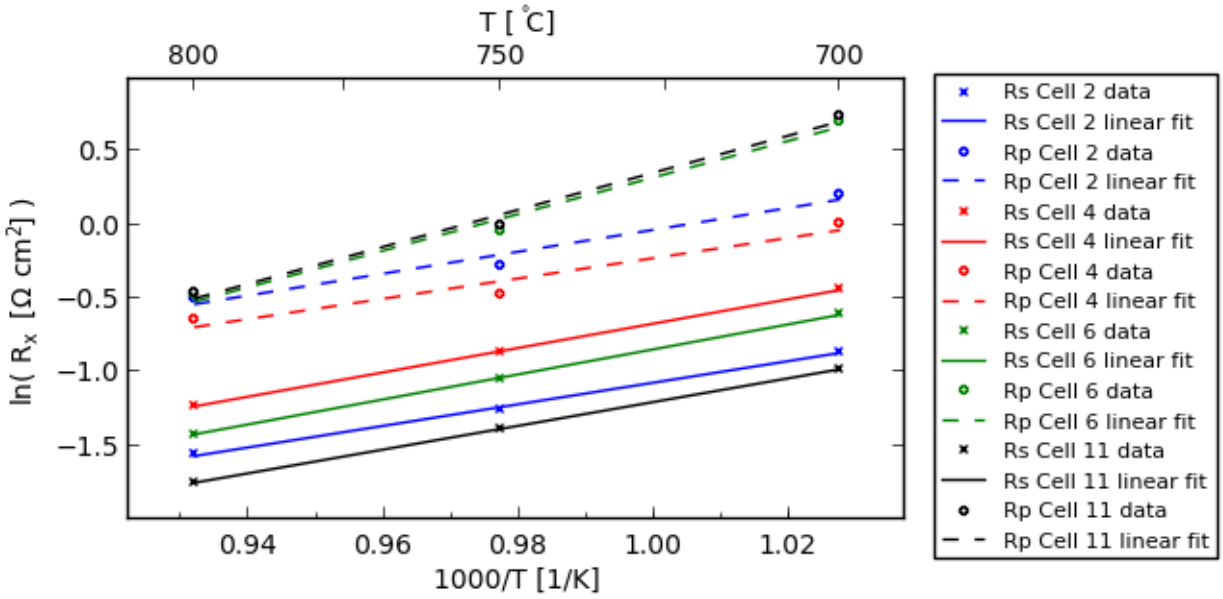

Figure 5 Arrhenius plot for the four cells of interest. Cell 2 – st.cer.coat, Cell 4 – CO LSM ws, Cell 6 – Cu and Cell 11 – Cu LSM ws

Table 2: Activation energies, E_a, for R_s and R_p for the different cells.

Cell	IC Coating	E_a for R_s	E_a for R_p
2	st.cer.coat.	0.630761 eV	0.639897 eV
4	Co LSM ws	0.711829 eV	0.592933 eV
6	Cu	0.731157 eV	1.06853 eV
11	Cu LSM ws	0.694298 eV	1.08289 eV

3.2 Long term degradation behaviour

The cell voltage history plot in Figure 6 shows the average cell voltage for the stack RUs. It can be split into four periods divided by shorter periods in which the data-logging system was off-line. In the middle of degradation period 1 the air humidification was initiated. . The galvanostatic test was continuous however, also in periods without data-logging. The average degradation rate is not constant during the test, but is greatest in period 1. When examining individual cell voltages (Figure 7), it is clear that RUs with different coating materials display very different degradation behaviour. In period 2 the degradation rate vary from cell 2 with -4.5 $mV{\cdot}kh^{-1}$ to cell 6 with -18.4 $mV{\cdot}kh^{-1}$. In period 4 the degradation rate vary from cell 2 with -1.1 $mV{\cdot}kh^{-1}$ to cell 11 with -84.2 $mV{\cdot}kh^{-1.}$ Cell 11 displays a progressive degradation trend (accelerating degradation) [11]. This may be due to effects such as spallation of the coating and/or loss of contact between cell and interconnects, leading to hot-spots and increased corrosion, which accelerates the degradation further. The RU with the standard ceramic coat (cell 2) displays a linear degradation in periods 2-4 after the initial nonlinear voltage drop in period 1.

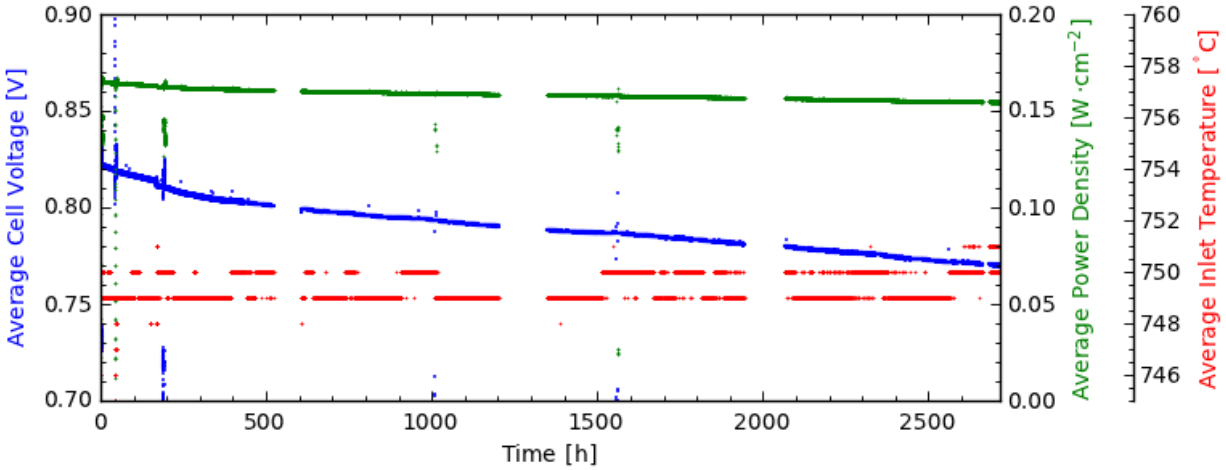

Figure 6: Overall stack performance during long term degradation.

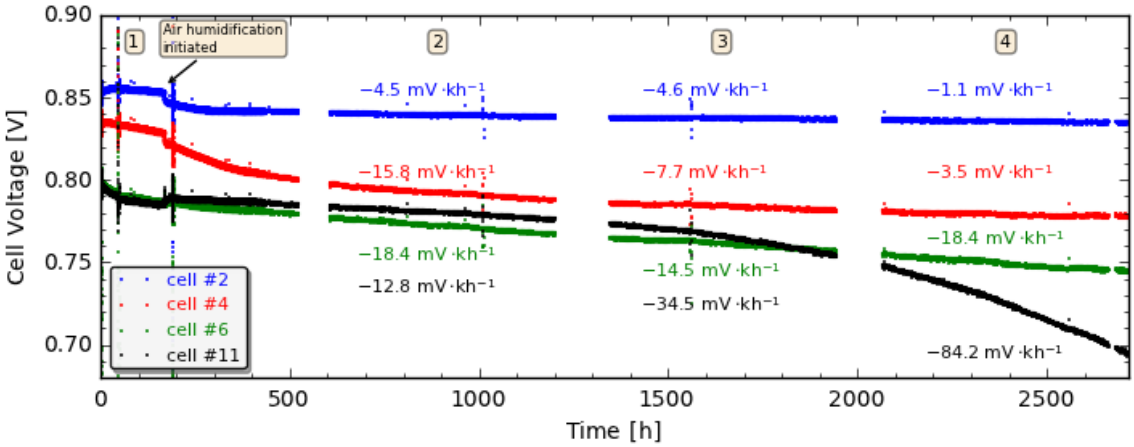

Figure 7: Cell voltages versus time. Annotation 1-4 corresponds to 4 different degradation periods. Cell 2 – st.cer.coat, Cell 4 – Co LSM ws, Cell 6 – Cu and Cell 11 – Cu LSM ws.

3.2.1 EIS monitoring

EIS spectra were recorded regularly on the four selected cells. **Figure 8** shows EIS spectra of the four cells just after the air humidification was initiated. The absolute value for Rs for the displayed impedance spectra is in the range between 5 to 8 mΩ.

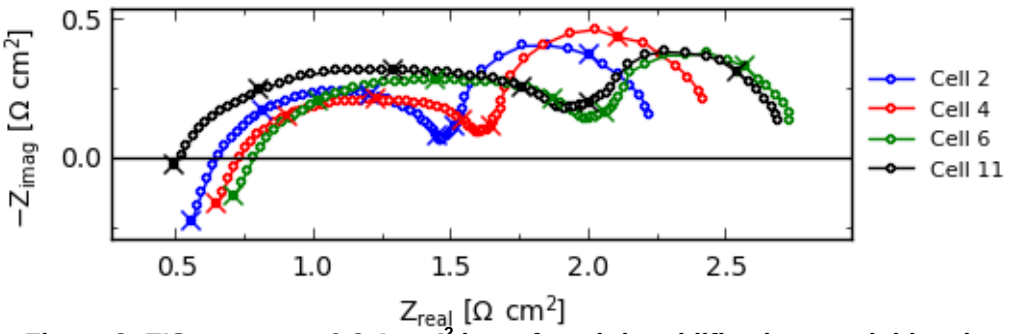

Figure 8: EIS spectra at 0.2 A cm^{-2} just after air humidification was initiated. Cell 2 – st.cer.coat, Cell 4 – Co LSM ws, Cell 6 – Cu and Cell 11 – Cu LSM ws. X corresponds to the frequencies 97 kHz, 9.7 kHz, 970 Hz, 97 Hz, 9.7 Hz and 0.97 Hz.

Figure 9 shows the resistance behaviour versus time for the series resistance, R_s and the polarisation resistance, R_p, as measured under current.

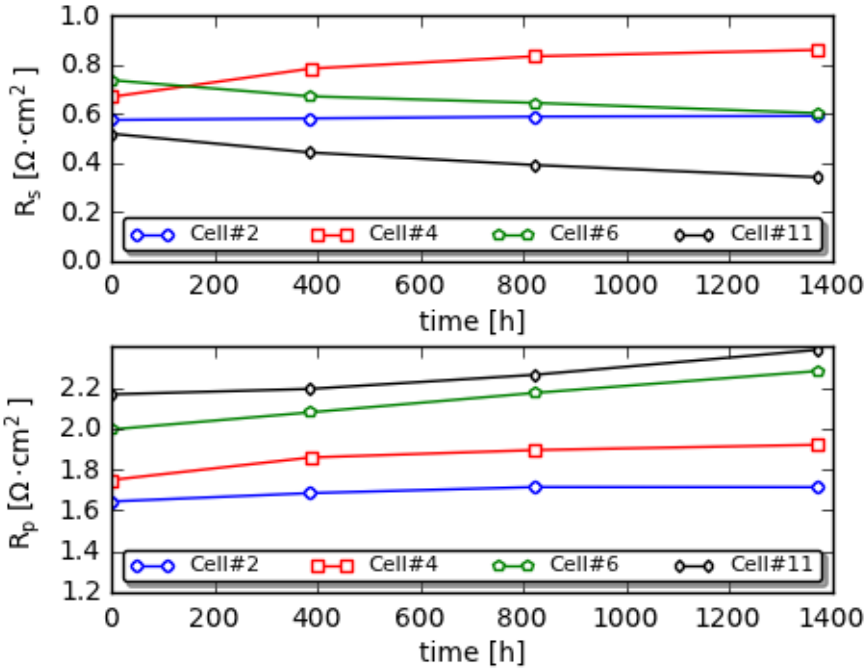

Figure 9: Resistance behaviour versus time. Cell 2 – st.cer.coat, Cell 4 – Co LSM ws, Cell 6 – Cu and Cell 11 – Cu LSM ws

3.2.2 Degradation mode tracking

Figure 10 shows the normalised polarisation resistance, R_p^0/R_p versus normalised series resistance, R_s^0/R_s where point (1,1) correspond to the initial situation. Plotting the evolution of normalised series and polarisation resistance starting at (1,1) provides useful visual information about the nature and extent of degradation. A degradation mode that mainly affects R_s like oxide layer growth appears as an almost horizontal progressing leftward with increasing extent of degradation [12]. Nickel coarsening (at shorter time-scales) [13], chromium poisoning [14] and/or water induced changes on the cathode side [15], is reflected as a vertical line down from (1,1) since it is mainly affects the R_p.

If the normalised resistance trajectory follows the 45 degree line it is an indication that a degradation process that changes the active area of the cell (*e.g.* delamination) may be dominating the degradation [12]. It is important to note that this way of plotting do not identify the degradation specifically, it only aids in identifying main types of degradation, R_s only, R_p only or usually both in various proportions.

Figure 10 illustrates that the degradation of cell 2 with the standard coating is characterised by occurring at the same rate for both R_s and R_p which could indicate a mechanism that changes the active area of the cell. For cell 4 one also observes that both resistances increase, but here Rs increases at a faster rate than R_p – this could indicate a combination of change the active area of the cell and an "R_s-only process" like e.g. oxide layer growth. Cell 6 and cell 11 behave differently; for these cells R_s decreases over time, but R_p, which dominate the total resistance increases. Figure 10 show the relative changes for R_s and R_p. For absolute changes of R_s and R_p see Figure 9.

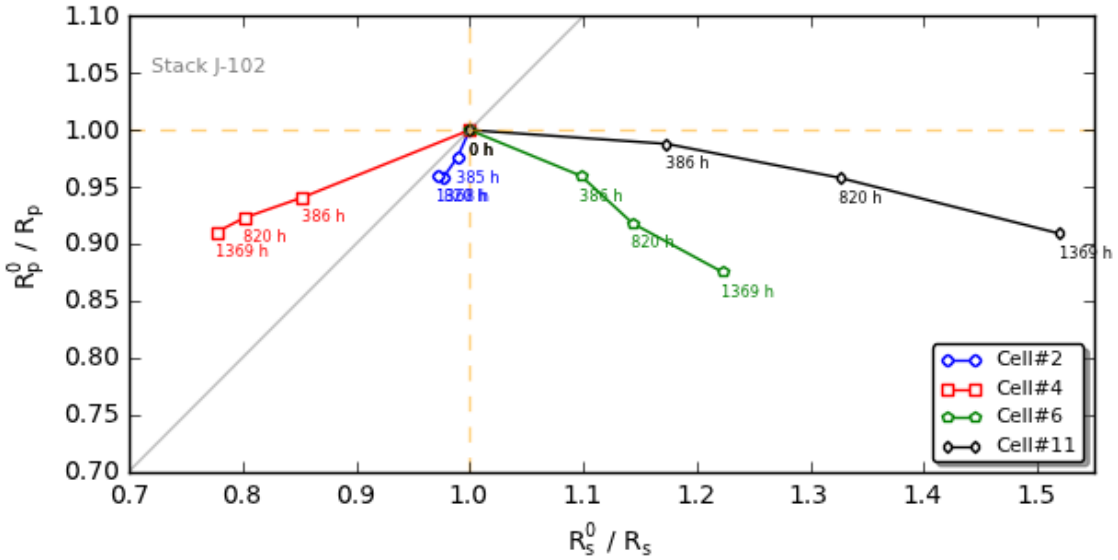

Figure 10: Degradation mode plot. Cell 2 – st.cer.coat, Cell 4 – Co LSM ws, Cell 6 – Cu and Cell 11 – Cu LSM ws.

4. Conclusions

A 13-cell experimental SOFC stack was tested during 2,500 hours of continuous operation with hydrogen as fuel with 52% fuel utilisation and constant current load (0.2 A cm-2) at 750˚C. Stack interconnects was coated with six different coatings to prevent chromium poisoning on the cathode side.

The stack geometry, in terms of current path and voltage probe placement was optimised for electrochemical impedance spectroscopy (EIS). The results illustrate that detailed EIS is possible on large area stacks and a de-convolution of the total loss into an ohmic and a non-ohmic part can be made.

The linear Kramers-Kronig Transform was used for data validation of the impedance spectra. Four cells were selected for detailed impedance analysis and degradation mode tracking. Cell 2 with the standard ceramic coating displayed the lowest long term degradation. The degradation of cell 4 with Co LSM wet sprayed coating was dominated by an increase of the series resistance with time, which could indicate that oxide layer growth was relatively rapid in the RU. Cell 6 and cell 11 showed increasing Rp values but decreasing Rs values. Analysis of all cell impedances in the stack (carried out at specific times only) show that the difference in behaviour between the four RU's does lie in the different interconnect coatings. Whereas the performance of the experimental coatings is unsatisfactory the experiment is successful in terms of characterisation – the EIS allowed a distinction to be made in terms of the degradation between the four RU types that is not possible from IV-data only.

Acknowledgements

The authors gratefully acknowledge Copenhagen Cleantech Cluster and EUDP under the project ENS-64010-0052 for financial support, Topsoe Fuel Cell A/S for material supply. Martin Nørby Nielsen from DTU Energy Conversion for improvements to our EIS measurement accuracy. Dr Christopher Graves from DTU Energy Conversion for use of the RAVDAV data analysis software package.

References

[1] U.S. Department of Energy. Distributed/stationary fuel cell systems 2011.

[2] Yokokawa H, Tu H, Iwanschitz B, Mai A. Fundamental mechanisms limiting solid oxide fuel cell durability. Journal of Power Sources 2008;182(2):400-412.

[3] Huang Q, Hui R, Wang B, Zhang J. A review of ac impedance modeling and validation in sofc diagnosis. Electrochimica Acta 2007;52(28):8144-8164.

[4] Comminges C, Fu QX, Zahid M, Steiner NY, Bucheli O. Monitoring the degradation of a solid oxide fuel cell stack during 10,000h via electrochemical impedance spectroscopy. Electrochimica Acta 2012;59:367-375.

[5] Lang M, Auer C, Eismann a, Szabo P, Wagner N. Investigation of solid oxide fuel cell short stacks for mobile applications by electrochemical impedance spectroscopy. Electrochimica Acta 2008;53(25):7509-7513.

[6] Ebbesen SD, Høgh J, Nielsen KA, Nielsen JU, Mogensen M. Durable soc stacks for production of hydrogen and synthesis gas by high temperature electrolysis. International Journal of Hydrogen Energy 2011;36(13):7363-7373.

[7] Dekker NJJ, van Wees JF, Rietveld G. Determination of the anode flow distribution in a sofc stack at nominal operating conditions by eis. ECS Transactions 2009;25(2):1871-1878.

[8] Hagen A, Barfod R, Hendriksen PV, Liu Y-L, Ramousse S. Degradation of anode supported sofcs as a function of temperature and current load. Journal of The Electrochemical Society 2006;153(6):A1165.

[9] Nielsen KA, Persson A, Beeaff D, Høgh J, Mikkelsen L, Hendriksen PV. Initiation and performance of a coating for countering chromium poisoning in a sofc-stackle. ECS Transactions 2007;7(1):2145-2154.

[10] Boukamp BA. A linear kronig-kramers transform test for immittance data validation. Journal of The Electrochemical Society 1995;142(6):1885.

[11] de Haart LGJ, Mougin J, Posdziech O, Kiviaho J, Menzler NH. Stack degradation in dependence of operation parameters; the real-sofc sensitivity analysis. Fuel Cells 2009;9(6):794-804.

[12] Gazzarri JI, Kesler O. Short stack modeling of degradation in solid oxide fuel cells. Journal of Power Sources 2008;176(1):155-166.

[13] Jiao Z, Shikazono N, Kasagi N. Study on degradation of solid oxide fuel cell anode by using pure nickel electrode. Journal of Power Sources 2011;196(20):8366-8376.

[14] Kornely M, Neumann A, Menzler NH, Leonide A, Weber A, Ivers-Tiffée E. Degradation of anode supported cell (asc) performance by cr-poisoning. Journal of Power Sources 2011;196(17):7203-7208.

[15] Lee D, Ahn S-J, Kim J, Moon J. Influence of water vapor on performance of co-planar single chamber solid oxide fuel cells. Journal of Power Sources 2010;195(19):6504-6509.